Amino Acids
https://doi.org/10.1007/s00726-018-2552-4

ORIGINAL ARTICLE

Leucine/Pd-loaded (5,5) single-walled carbon nanotube matrix as a novel nanobiosensors for in silico detection of protein

Mehdi Yoosefian[1] · **Nazanin Etminan**[2]

Received: 14 July 2017 / Accepted: 8 March 2018

Abstract
We have designed a novel nanobiosensor for in silico detecting proteins based on leucine/Pd-loaded single-walled carbon nanotube matrix. Density functional theory at the B3LYP/6-31G (d) level of theory was realized to analyze the geometrical and electronic structure of the proposed nanobiosensor. The solvent effects were investigated using the Tomasi's polarized continuum model. Atoms-in-molecules theory was used to study the nature of interactions by calculating the electron density $\rho(r)$ and Laplacian at the bond critical points. Natural bond orbital analysis was performed to achieve a deep understanding of the nature of the interactions. The biosensor has potential application for high sensitive and rapid response to protein due to the chemical adsorption of L-leucine amino acid onto Pd-loaded single-walled carbon nanotube and reactive functional groups that can incorporate in hydrogen binding, hydrophobic interactions and van der Waals forces with the protein surface in detection process.

Keywords Nanoreceptor · Protein detection · Carbon nanotube · Chemical sensing

Introduction

Biological process monitoring has an increasing important role in clinic, diagnostic, medical, therapeutics, healthcare and drug delivery fields. The biosensors are the self-contained integrated devices that utilize a biological recognition element in direct contact with a transducer element to convert biological data to electrical signal, providing specific quantitative or semi-quantitative analytical information (Nambiar and Yeow 2011). The first biosensor was described in 1962 by Clark to qualify glucose concentration with a combination of glucose oxidase enzyme and electrochemical oxygen in aqueous media (Clark and Lyons 1962). Miniaturization of biosensor approach by the combination of biological components with nanomaterials seems to be an important developmental feature of in vivo application of biosensors (Ye and Ju 2005). Carbon nanomaterials (CNs) from zero dimension (0-D) to three dimension (3-D) have promising applications in different fields including nanoelectronics (Cao et al. 2013), energy storage and field emission display (Liu et al. 2012), biomedical applications (e.g., theranostics) (Liu and Liang 2012), biological and chemical sensors (Yoosefian 2017; Yoosefian and Etminan 2016a). Carbon nanotubes (CNTs), discovered by Iijima in 1991 (Iijima 1991), are graphite sheets rolled up into a nanoscale tube. CNTs can be divided into two main groups: single-walled carbon nanotubes (SWCNTs) and multi-walled carbon nanotubes (MWCNTs). CNTs have attracted increasing research interest due to their unique structural, electronic and chemical properties. CNTs with good electrical conductivity, high thermal and mechanical stability and with slow oxidation kinetics and high electrocatalytic activity can provide real-time information of metabolite compound monitoring (Balasubramanian and Burghard 2006). The biocompatibility and possibility of covalent/non-covalent chemical functionalization of carbon nanotubes has been regarded them as biosensor platforms in biotechnology, chemical and environmental researches.

Handling Editor: H. S. Sharma.

✉ Mehdi Yoosefian
m.yoosefian@kgut.ac.ir

Nazanin Etminan
netminan2015@gmail.com

[1] Department of Nanotechnology, Graduate University of Advanced Technology, Kerman, Iran

[2] Chemistry Department, University of Payam-noor, 19395-4697 Tehran, Iran

Published online: 14 March 2018

σ–π rehybridization and high specific surface of CNTs facilitate the direct electron transfer, doping and molecular adsorption and allow the load of high density electrochemical active biological agents to improve electrochemical signals. Functional adsorbents could affect the electron transfer rate and electrocatalytic activity of CNTs. These nanostructured platforms decrease the response time and increase the sensitivity of biosensor. Nano-sized biosensors are very important in biological sensors because important biomacromolecule structures are in the range of 1–1000 nm (Jianrong et al. 2004). SWCNTs can be functionalized through doping, decorating or defecting with impurity atoms to improve the adsorption feature. The shift in Fermi level with dopant metal can modify the reactivity and the electronic properties of SWCNT (Yoosefian and Etminan 2016b). Because of the hydrophobic surface of pristine SWCNT, functionalized nanomaterials could be good candidates in bionanosensor platform because of the biocompatibility and aqueous solubility (Etminan et al. 2016). Molecular recognition that deals with molecular complexes, formed through non-covalent interactions such as hydrogen binding, hydrophobic interactions, van der Waals forces and π–π stacking. Detection occurs through the binding event at the surface of the receptor and target on the surface of nanobiosensor. Amino acids are biocompatible biomolecules and highly water soluble. The affinity between protein and analyte is the basic motivation in our study to introduce the L-leucine (Leu) aliphatic amino acid as a biological receptor on SWCNT transducer platform. Therefore, an attempt has been made to study the detailed theoretical DFT investigation of leucine/Pd-loaded single-walled carbon nanotube (Leu–Pd/SWCNT) matrix as new novel nanobiosensors.

The performance of a biosensor is not only depends on molecular structure but also affected by the environmental effects and mostly the solvents. The main objective of this study is to understand the reactivity and stability of leucine aliphatic amino acid as the recognition element and the transition metal-doped carbon nanotube as the enhanced physical transducer in the new novel nanobiosensor.

The calculated results with DFT/B3LYP/6-31G (d) are valuable, which provide insights into geometrical parameters and the stability and reactivity descriptors. The natural bond orbital (NBO), frontier molecular orbital (FMO) and quantum theory atoms in molecule (QTAIM) analysis have been also performed. Furthermore, molecular electrostatic potential surfaces (MEPS) and density of states (DOS) of the nanobiosensor have been constructed. Solvent effects were investigated in different solvents (water, DMSO, ethanol, acetone and CCl_4) using the polarized continuum model (PCM).

Computational details

The quantum theoretical calculations were performed at DFT level using the Gaussian 09 program package (Frisch et al. 2010). The 5,5 armchair single-walled carbon nanotube with 69 carbon atoms and 20 hydrogen atoms and a palladium atom were selected as sensing platform. The geometries were optimized at the DFT/B3LYP level of theory employing the 6-31G(d) basis set (Becke 1993; Lee et al. 1988). The QTAIM calculations were done by AIM2000 program to analyze the interactions via the electron densities and their Laplacian at the bond critical points (BCPs) (Bader 1998). DFT-based stability and reactivity descriptors were calculated by the molecular orbital calculations. The adsorption energy of L-amino acid (a.a) onto Pd/SWCNT due to different conformational orientations was calculated as defined

$$E_{ads} = E_{Leu-Pd/SWCNT} - E_{Pd/SWCNT} - E_{Leu}, \quad (1)$$

where $E_{Leu-Pd/SWCNT}$ is the total energy of the Pd/SWCNT with L-leucine (Leu) molecule and $E_{Pd/SWCNT}$ and E_{Leu} are the total energies of Pd/SWCNT and Leu molecule in relax geometry, respectively. Negative adsorption energy indicates the stable formed complexes and the positive adsorption energy referred to the local minima. All optimized geometries were verified to be local minima since no imaginary frequencies were found in frequency calculations.

For the Leu–Pd/SWCNT system, we investigated various possible adsorption geometries. Among them, two representative configurations, in which the Pd-doped SWCNT is close to amine site (Complex 1) and carboxyl site (Complex 2) of Leu molecule were the most stable conformes. The perpendicular direction of functional groups to SWCNT was considered to reduce the unfavorable interactions. The frontier molecular orbital (FMO) analysis is employed to calculate the DFT-based global reactivity indices (Parr et al. 1999; Pearson 1988):

$$\mu = \left(\frac{\partial E}{\partial N}\right)_{V(r)}, \quad (2)$$

$$\eta = \left(\frac{\partial^2 E}{\partial N^2}\right)_{V(r)}. \quad (3)$$

Result and discussion

Geometrical structure

As only L-amino acids are manufactured in cells and incorporated into protein; the adsorption of a single aliphatic L-leucine molecule onto the Pd/SWCNT was investigated via two possible active adsorption sites, including amine and carboxylic acid site on open-edged Pd-doped (5,5)

SWCNT, ($C_{69}H_{20}Pd$). Full-optimized molecular structure was calculated at B3LYP/6-31G(d) level. The electronic wave functions were expanded in the DGDZVP atomic basis function for Pd atom. Geometry optimization was conducted without any symmetry constrain. The diameter of SWCNT is 7.17 Å. Figure 1 shows the structure of Pd/SWCNT. A central C atom in the side wall of SWCNT is replaced by a Pd atom to model-doped SWCNT. In comparison with the corresponding carbon–carbon bonds (1.42 Å) in pristine SWCNT, the Pd–carbon bonds are longer and the Pd atom protrudes out off the wall surface because of the much larger Pd atom radius. The vertical Pd–C40 bond length is 2.063 Å and the slant Pd–C45 and Pd–C49 bond lengths are 1.974 and 1.974 Å, respectively. The longer bond length indicates that the vertical bond is weaker. The optimized geometry of Leu amino acid is depicted in Fig. 1.

Two representative adsorption configurations of interacted Leu with Pd/SWCNT (complex 1 and complex 2, respectively) are shown in Fig. 2 by panels I–IV.

The cylindrical structure of Pd-SWCNT is not significantly distorted after the Leu adsorption. However, the interactions have relatively significant influence on slant and vertical Pd–C bonds. The maximum elongation of Pd–C in Pd-SWCNT is about 0.0282 Å. The lengthening of N–H bonds in complex 1 is about 0.0018 Å and the lengthening of C–O bond in complex 2 is about 0.0184 Å which indicates the intermolecular interactions. Some of important geometrical parameters after full optimization are listed in Table 1. The corresponding interaction distances of Pd…N and Pd…O is 2.3173 Å and 2.2787 Å, respectively. Based on the calculated data, adsorption energy (E_{ads}) of complex 1 and complex 2 is − 105.02 and − 78.76 k $Jmol^{-1}$, respectively. These extraordinary E_{ads} indicate that Leu undergoes

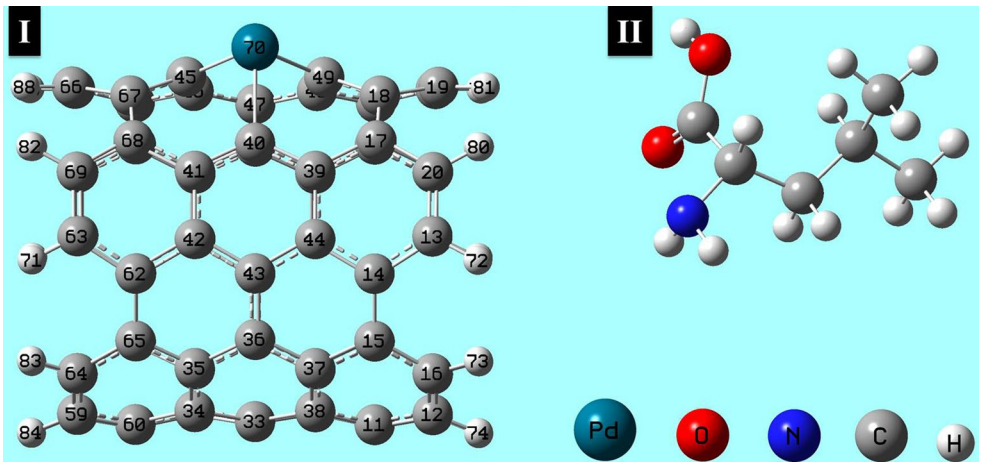

Fig. 1 The optimized geometries of (I) Pd-doped SWCNTs in side view and (II) L-leucine amino acid

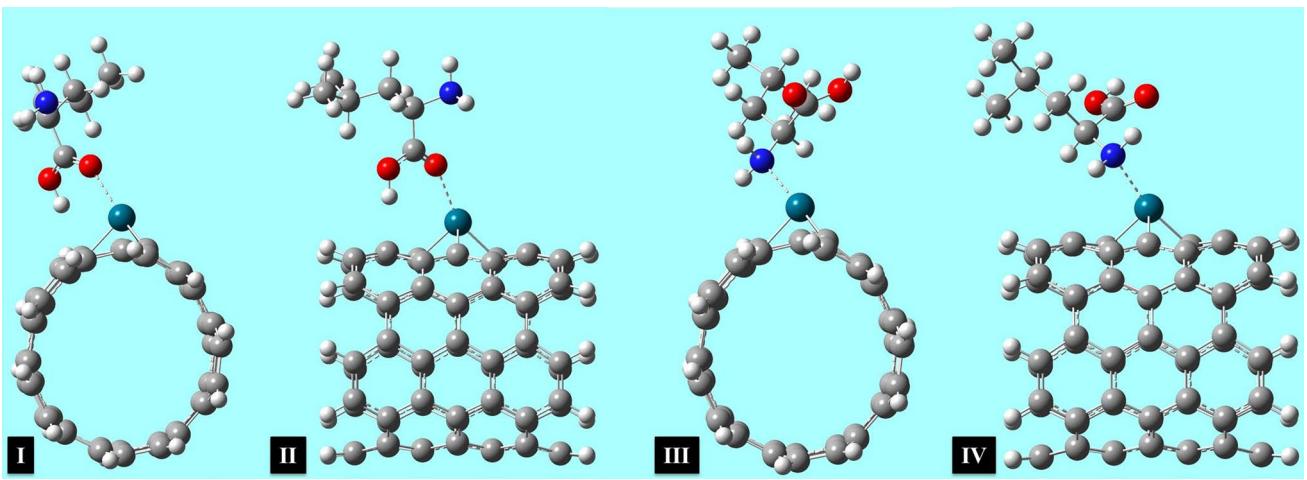

Fig. 2 Optimized geometry of Leu–Pd/SWCNT complexes; panels (I) from carboxylic acid site in top view, (II) from carboxylic acid site in side view, (III) from amine site in top view and (IV) from amine site in side view

Table 1 Optimized interaction distance (ID in Å), topological parameters (in a.u.) and the adsorption energies (E_{ads} in kJ/mol) of the Leu–Pd/SWCNT nanobiosensor in various media

Media	Complex 1				Complex 2			
	ID	ρ_{BCP}	$\nabla^2\rho_{BCP}$	E_{ads}	ID	ρ_{BCP}	$\nabla^2\rho_{BCP}$	E_{ads}
Water	2.3268	0.05798	0.23996	− 73.88	2.3223	0.04445	0.22349	− 44.86
DMSO	2.3206	0.05798	0.24013	− 74.66	2.3214	0.04457	0.2242	− 45.88
Ethanol	2.3204	0.05799	0.24051	− 76.30	2.3194	0.04481	0.22575	− 47.96
Acetone	2.3203	0.05799	0.24067	− 76.99	2.3185	0.04491	0.22644	− 48.82
CCl4	2.3174	0.05817	0.24533	− 96.69	2.29	0.04864	0.25046	− 71.45
Gas phase	2.3173	0.05811	0.24639	− 105.02	2.2787	0.05031	0.26103	− 78.86

chemical adsorption on Pd/SWCNT and also proved this platform a stable nanobiosensor.

AIM analysis

Topological feature of electron density $\rho(r)$ is associated with a critical point (CP) where $\nabla^2\rho(r_c)=0$. The line of maximum charge density that links the nuclei is called a bond path and the (3, − 1) CP is referred to as a bond critical point. A (3, − 1) CP has the property of accumulating electron density at the CP in the perpendicular plane to internuclear axis between a pair of nuclei which are considered to be bonded to one another (Bader 1998).

The presence of the bond critical points and bond paths as the first criterion of bond formation is shown in the molecular graphs of the complexes. Figure 3 shows the linear bond paths in molecular graphs and the contour maps.

The calculated $\rho(r)$ and its second derivative $\nabla^2\rho(r_c)$ exhibit the nature of molecular bonds. The properties of the Laplacian of the electron density, that was first used by Koch and Popelier, determine where the electron density is locally concentrated, $\nabla^2\rho(r_c)<0$ and where the electron density is locally depleted, $\nabla^2\rho(r_c)>0$. Our results show the negative values of the Laplacian which attributed to closed-shell interactions. Results are listed in Table 1.

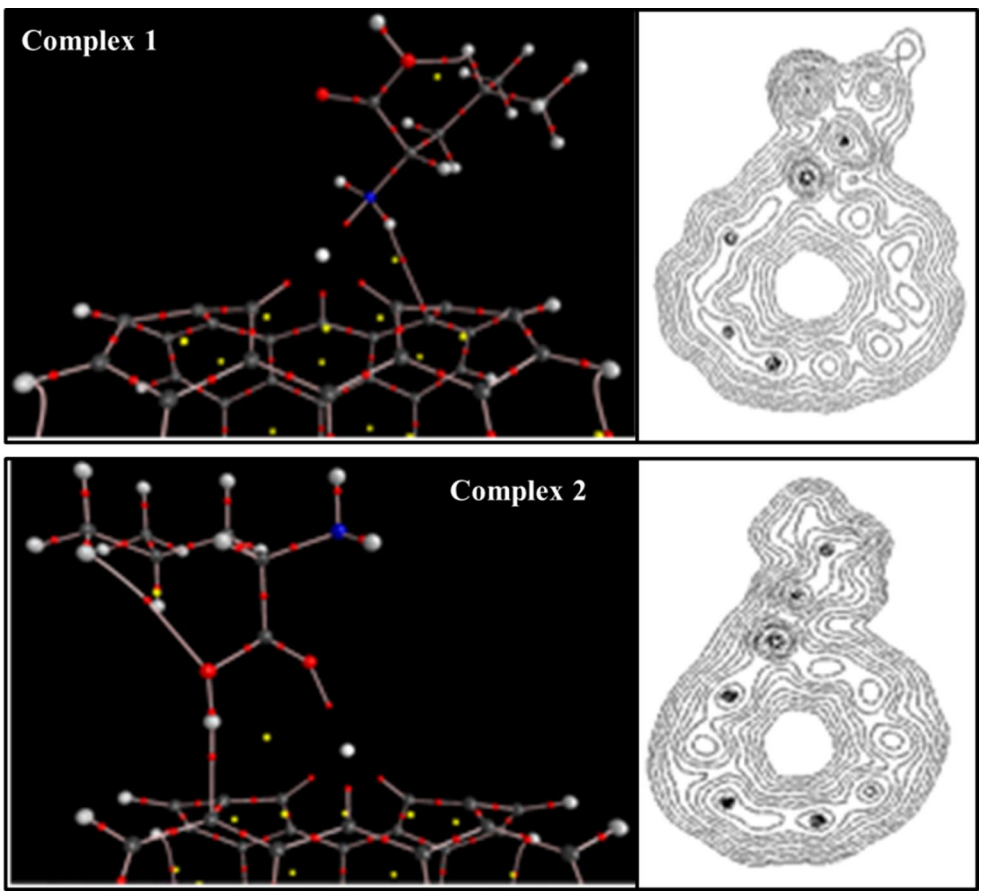

Fig. 3 Contour maps (right) and molecular graphs (left) of the studied complexes of Leu–Pd/SWCNT

Table 2 NBO analysis of Leu–Pd/SWCNT complexes: second-order perturbation energy ($E^{(2)}$ in kcal/mol) of some important orbital interactions (numbering as in panel I, Fig. 1)

Complex 1			Complex 2		
Donor	Acceptor	$E^{(2)}$	Donor	Acceptor	$E^{(2)}$
σN–H	LP*(7)Pd70	3.12	LP (2) O	LP*(7)Pd70	16.16
LP (1) N	LP*(5)Pd70	5.29	LP (2) O	LP*(5)Pd70	11.59
LP (1) N	LP*(7)Pd 70	6.30	LP (1) O	LP*(7)Pd70	8.17
LP (1) N	σ*C49 -Pd70	24.53	LP (1) O	LP*(6)Pd70	12.14

NBO analysis

If a CNT is semiconducting in nature, charge transfer can lead to changes in electrical conductance of the CNT. To elucidate the charge transfer between the Pd/SWCNT and Leu molecule, NBO calculation was carried out. The NBO method is also applied here to evaluate the second-order perturbation theory interaction energy, $E^{(2)}$. The donor–acceptor interactions have been evaluated by the second-order Fock matrix. The stabilization energy, $E^{(2)}$, associated with the delocalization of donor (i) to acceptor (j) is estimated as (Reed et al. 1988; Raissi et al. 2012)

$$E^{(2)} = \Delta E_y = q_i \frac{F^{(2)}(ij)}{\varepsilon_i - \varepsilon_j}. \quad (4)$$

Table 2 presents the NBO analysis of the strong intermolecular charge transfer interactions.

The results of the NBO analysis illustrate that in the Leu–Pd/SWCNT system the lone pairs of N and O atoms

Table 3 The highest occupied molecular orbital (HOMO) energy, the lowest unoccupied molecular orbital (LUMO) energy, energy gap and DFT-based chemical reactivity descriptors (all values in eV) of Leu–Pd/SWCNT and its components

Molecular parameters	Pd/SWCNT	Leu	Complex 1	Complex 2
EHOMO	− 4.155	− 6.373	− 3.912	− 4.047
ELUMO	− 2.543	0.169	− 2.236	− 2.344
ΔE HOMO–LUMO	1.612	6.542	1.677	1.703
Ionization potential (IP)	4.155	6.373	3.912	4.047
Electron affinity (EA)	2.543	− 0.169	2.236	2.344
Chemical potential (μ)	− 3.349	− 3.102	− 3.074	− 3.195
Chemical hardness (η)	0.806	3.271	0.838	0.852
Chemical softness (S)	0.620	0.153	0.596	0.587
Global electrophilicity index (ω)	6.958	1.471	5.637	5.994

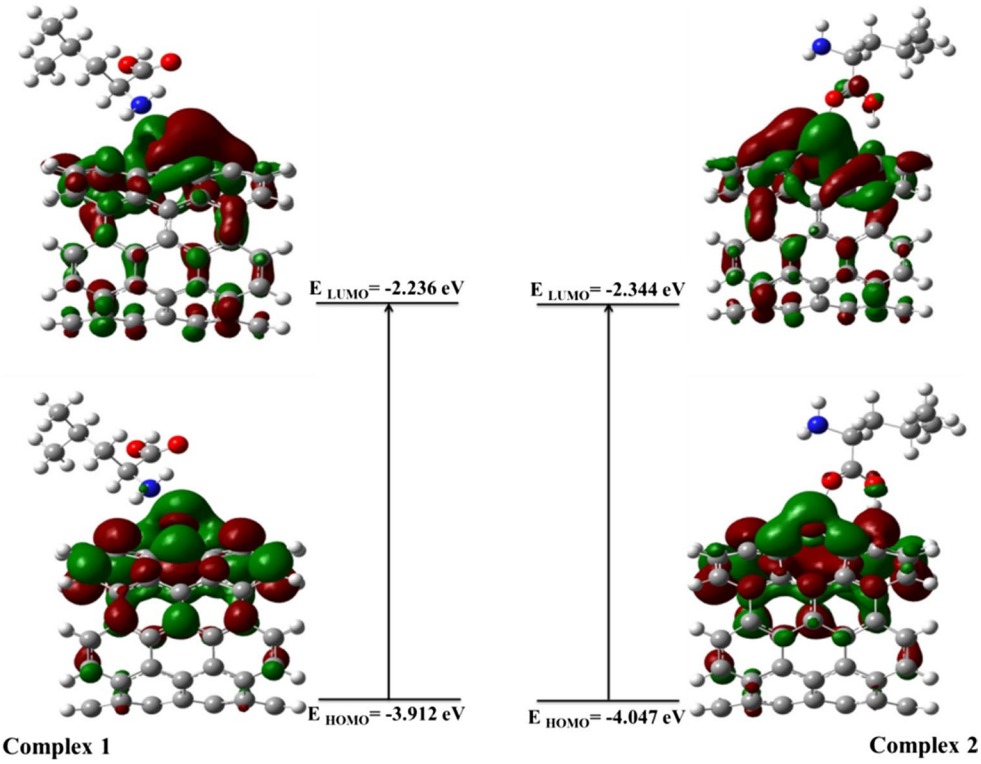

Fig. 4 HOMO and LUMO compositions of the frontier molecular orbital for complexes of Leu–Pd/SWCNT

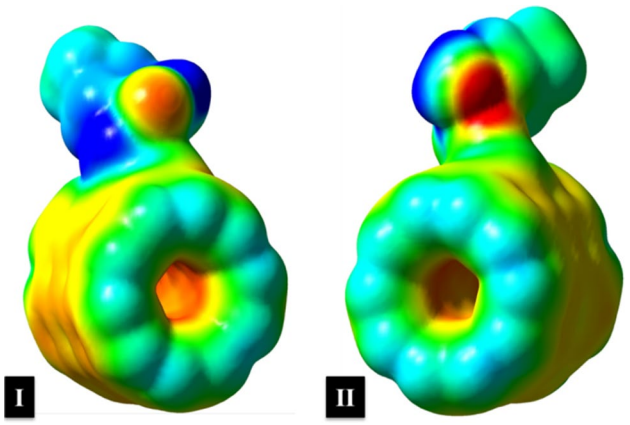

Fig. 5 The molecular electrostatic potential graphic representations for complexes of Leu–Pd/SWCNT

participate as a donor and the Lp*(Pd) and σ*(C49–Pd70) interaction as the acceptors are the strongest intramolecular charge transfer interactions. Acceptable charge transfers and the adsorption energies indicate the chemical adsorption process.

Molecular orbital analysis

Another important criterion to evaluate the sensing performance is the frontier molecular orbital theory. The highest occupied molecular orbital (HOMO) and the lowest unoccupied molecular orbital (LUMO) are involved in chemical reactivity. The HOMO is the highest energy orbital that could be simply donating electron density to form a bond, and the LUMO is the lowest lying empty orbital that energetically could add more electrons into this orbital. The HOMO–LUMO energy gap, which is defined as the HOMO–LUMO energy separation of a molecule, is a simple indicator of kinetic stability. Conceptual DFT-based reactivity and stability descriptors are calculated and presented in Table 3. A large HOMO–LUMO gap implies high kinetic stability and low chemical reactivity. Our results reveal that the HOMO–LUMO energy gap of complex 2 is higher than that of complex 1 so it is kinetically more stable. The chemical hardness of complex 1 is lower which indicates the higher reactivity. The HOMO–LUMO orbitals of Leu–Pd/SWCNT are shown in Fig. 4. The larger electron projection could be seen over the doping site of Pd/SWCNT.

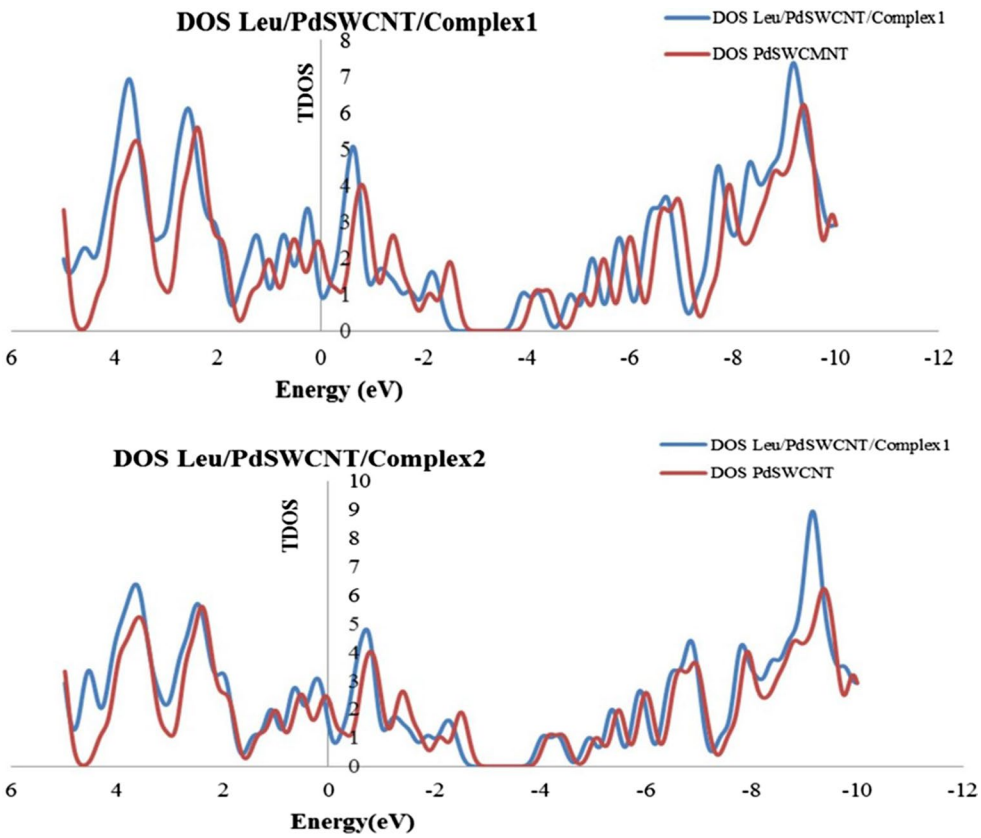

Fig. 6 Calculated electronic DOSs for the Pd/SWCNT and complexes of Leu–Pd/SWCNT

Molecular electrostatic potential surfaces (MESP)

Molecular electrical potential surfaces (MEPS) illustrate three-dimensional charge distributions of molecules. MPES allow us to visualize variable charged regions of Leu–Pd/SWCNT. Knowledge of the charge distributions can be used to determine how proteins interact with the amino acid adsorbed onto the Pd/SWCNT. It also predicts the behavior of molecules and visualizes the size and the shape of molecules. To interpret the electrostatic potential energy data, a color spectrum is used in which the red color presents the lowest electrostatic potential energy value and the blue color presents as the highest. All color spectra could be found in the surface of the system which facilitates the electrophilic and nucleophilic interactions of the designed nanobiosensor with the protein surface. The molecular electrostatic potential graphic representations for complexes are depicted in Fig. 5. The negative (red and yellow color) regions of MEPS are related to electrophilic reactivity and the positive regions (blue color) are related to nucleophilic reactivity.

Table 4 The calculated total energies (E_{tot} in Hartree), dipole moments (DM in Debye) and the stabilization energies (E_{stab} in k J/mol) of the Leu–Pd/SWCNT and its components in various media

Media	Leu	Pd/SWCNT	Complex 1	Complex 2
Gas phase				
E_{tot}	− 441.6744	− 7580.9931	− 8022.7081	− 8022.6997
DM	1.949	2.168	7.809	5.594
Water (ε = 78.54)				
E_{tot}	− 441.6846	− 7581.0292	− 8022.7420	− 8022.7309
DM	3.396	9.035	13.616	9.604
E_{stab}	− 26.712	− 94.948	− 88.837	− 81.923
DMSO (ε = 46.7)				
E_{tot}	− 441.6844	− 7581.0283	− 8022.7412	− 8022.7302
DM	3.380	8.829	13.458	9.481
E_{stab}	− 26.225	− 92.529	− 86.710	− 80.043
Ethanol (ε = 24.55)				
E_{tot}	− 441.684	− 7581.0264	− 8022.7395	− 8022.7287
DM	3.338	8.404	13.142	9.247
E_{stab}	− 25.185	− 87.636	− 82.417	− 76.189
Acetone (ε = 20.7)				
E_{tot}	− 441.6839	− 7581.0257	− 8022.7388	− 8022.7281
DM	3.322	8.233	13.011	9.151
E_{stab}	− 24.725	− 85.595	− 80.613	− 74.550
CCl4 (ε = 2.24)				
E_{tot}	− 441.6784	− 7581.0051	− 8022.7203	− 8022.7106
DM	2.278	4.017	9.838	6.860
E_{stab}	− 10.327	− 31.503	− 31.820	− 28.690

Density of state (DOS)

Significant difference in frontier molecular orbitals results from the large charge transfer which affects the density of states near the Fermi level. The total DOS of the complexes were predicted to elucidate the electronic properties and the influence of Leu adsorbed on the Pd/SWCNT and also the Leu–Pd/SWCNT. By comparison with the Pd/SWCNT, the bong gap of the Leu–Pd/SWCNT increases. A slightly left move happens to the DOSs of the complexes around the Fermi level. These changes in the DOSs would result in the conductance change of functionalized nanotube (see Fig. 6).

Solvent effect

Compared with the gas phase, the interactions with the solvent change the molecular properties due to the perturbations of the molecular system in the solvent (Yoosefian et al. 2016; Yoosefian and Mola 2015; Mammino and Kabanda 2009). The self-consistent reaction field (SCRF) theory has been applied to describe the solvent effects based on polarizable continuum model (PCM) (Barone et al. 1997). In the present study, we have investigated the solvent effects on the geometry and electronic properties of the purposed nanobiosensor in water, DMSO, ethanol, acetone and carbon tetrachloride using the DFT/B3LYP with the 6-31G (d) basis set in combination with the PCM model. The calculated values of total energies, dipole moments and the stabilization energies are reported in Table 4. Results show that the total energy of the systems in solvent is lower than that in the gas phase, and the stabilization energies depend on the size of the electric permittivity of the solvent. It can be seen that by increasing the electric permittivity of the solvent, the total energy values of the system shifts to lower values. The calculated results show that Leu–Pd/SWCNT system has the largest dipole moment in water. Thus, the polarity of the titled nanobiosensor increases with the increasing solvent polarity which is due to the induced effects of the solvent. The electric field applied to the solute by the solvent leads to net stabilization of the system.

Optimized geometric and topological parameters in different solvents show that by increasing the solvent polarity the interaction distances increase and the electron charge density decreases. It is clear that the adsorption energy of the Leu onto the Pd/SWCNT decreases by increasing the solvent polarity because of the nonpolar nature of the system. Results are listed in Table 1.

Table 5 indicates that solvents have effective effects on the DFT-based reactivity and stability descriptors. Ongoing from the gas phase to polar solvents, the HOMO and LUMO energies and the energy gap decrease. Therefore, the chemical hardness decreases and the more chemical reactive

Table 5 The highest occupied molecular orbital (HOMO) energy, the lowest unoccupied molecular orbital (LUMO) energy, energy gap and DFT-based chemical reactivity descriptors (all values in eV) of complex 1 in various media (values in parentheses refer to complex 2)

Molecular parameters	Water	DMSO	Ethanol	Acetone	CCl4
EHOMO	− 4.038 (− 4.175)	− 4.032 (− 4.168)	− 4.020 (− 4.156)	− 4.015 (− 4.151)	− 3.935 (− 4.070)
ELUMO	− 2.408 (− 2.480)	− 2.399 (− 2.473)	− 2.381 (− 2.459)	− 2.376 (− 2.453)	− 2.263 (− 2.362)
ΔE HOMO–LUMO	1.631 (1.695)	1.633 (1.696)	1.638 (1.698)	1.639 (1.698)	1.672 (1.708)
Ionization potential (IP)	4.038 (4.175)	4.032 (4.168)	4.020 (4.156)	4.015 (4.151)	3.935 (4.070)
Electron affinity (EA)	2.408 (2.480)	2.399 (2.473)	2.381 (2.459)	2.376 (2.453)	2.263 (2.362)
Chemical potential (μ)	− 3.223 (− 3.328)	− 3.215 (− 3.321)	− 3.201 (− 3.307)	− 3.196 (− 3.302)	− 3.099 (− 3.216)
Chemical hardness (η)	0.815 (0.847)	0.816 (0.848)	0.819 (0.849)	0.820 (0.849)	0.836 (0.854)
Chemical softness (S)	0.613 (0.590)	0.612 (0.590)	0.610 (0.589)	0.610 (0.589)	0.598 (0.586)
Global electrophilicity index (ω)	6.371 (6.534)	6.331 (6.503)	6.253 (6.444)	6.230 (6.422)	5.743 (6.056)

Table 6 NBO analysis of Leu–Pd/SWCNT complexes in various media: second-order perturbation energy ($E^{(2)}$ in kcal/mol) of some important orbital interactions (numbering as in panel I, Fig. 1) in various media

	Donor	Acceptor	Water	DMSO	Ethanol	Acetone	CCl4
Complex 1	LP (1) N	LP (1)C 40	2.69	2.67	2.68	2.66	2.68
	LP (1) N	LP*(4)Pd	14.65	14.72	14.83	14.89	14.83
	LP (1) N	LP*(5)Pd	20.19	19.92	19.39	19.11	19.39
	LP (1) N	LP*(6)Pd	4.89	5.28	6.03	6.42	6.03
Complex 2	LP (1) O	LP*(4)Pd	24.41	24.39	24.33	24.31	4.32
	LP (2) O	LP*(4)Pd	20.71	20.74	20.79	20.8	17.12
	LP (2) O	LP*(5)Pd	3.27	3.41	3.72	3.87	2.70
	LP (2) O	σ*C49–Pd	9.38	9.39	9.42	9.43	6.46

system would be in water medium. It can be seen that the electrophilicity index increases with the increasing solvent polarity.

The calculated values of NBO analysis of second-order perturbation theory interaction energy, $E^{(2)}$, between the donor–acceptor orbitals of optimized complexes of Leu–Pd/SWCNT in various media are listed in Table 6. Results indicate that there are higher second-order perturbation theory interaction energies in more polar medium in complex 1 and the reverse trend in complex 2.

It can be seen that solvent effect induced slight changes in DOSs of the titled nanobiosensor due to the nature of PCM model that the solute is placed in a cavity representing the space occupied by the solute and the solvent electrostatic field, called reaction field is calculated. So, in solvents with nearly close dielectric constant, not important changes in DOSs would result.

Conclusion

In this work, a complete structural and electronic investigation of Leu–Pd/SWCNT as a new nanobiosensor for protein detection along with AIM, NBO, MPES and FMO analysis have been carried out with B3LYP method and 6-31G(d) basis set. It is found that strong chemical bond formed between Pd and amine group and also carboxylic acid with adsorption energies of 99.40 and 77.3 k $Jmol^{-1}$. Detailed analysis of the electronic properties of the adsorbed Leu aliphatic amino acid on Pd/SWCNT was studied in terms of DOS. This adsorption process influences the electronic states and changes the band gap. The chemical stability and reactivity of the studied systems have been considered in terms of the conceptual DFT-based descriptors. Complex 1 is more reactive system with less electrophilicity index. Since the solvation may change the electronic structure of the complexes, full geometry optimization and all mentioned analysis were performed in five different solvents (water, DMSO, ethanol, acetone and CCl_4). Our results confirm that the complexes are more reactive in water medium with relatively higher charge transfers. Our results verify that Leu amino acid could be a suitable bioreceptor due to the reactive functional groups that can incorporate in hydrogen binding, hydrophobic interactions and van der Waals forces with the protein surface in detection process.

Acknowledgements The authors wish to thank Graduate University of Advanced Technology, Kerman, Iran, for their support.

Compliance with ethical standards

Conflict of interest The authors declare that they have no conflict of interest.

Informed consent Informed consent was obtained from all individual participants included in the study.

Ethical approval All procedures performed in studies involving human participants were in accordance with the ethical standards of the institutional and/or national research committee and with the 1964 Helsinki declaration and its later amendments or comparable ethical standards.

References

Bader RF (1998) A bond path: a universal indicator of bonded interactions. J Phys Chem A 102(37):7314–7323

Balasubramanian K, Burghard M (2006) Biosensors based on carbon nanotubes. Anal Bioanal Chem 385(3):452–468

Barone V, Cossi M, Tomasi J (1997) A new definition of cavities for the computation of solvation free energies by the polarizable continuum model. J Chem Phys 107(8):3210–3221

Becke AD (1993) Density-functional thermochemistry. III. The role of exact exchange. J Chem Phys 98:5648

Cao Q, S-j Han, Tulevski GS, Zhu Y, Lu DD, Haensch W (2013) Arrays of single-walled carbon nanotubes with full surface coverage for high-performance electronics. Nat Nanotechnol 8(3):180–186

Clark LC, Lyons C (1962) Electrode systems for continuous monitoring in cardiovascular surgery. Ann N Y Acad Sci 102(1):29–45

Etminan N, Yoosefian M, Raissi H, Hakimi M (2016) Solvent effects on the stability and the electronic properties of histidine/Pd-doped single-walled carbon nanotube biosensor. J Mol Liq 214:313–318

Frisch M, Trucks G, Schlegel H, Scuseria G, Robb M, Cheeseman J, Scalmani G, Barone V, Mennucci B, Petersson G (2010) Gaussian 09, Rev B 01. Gaussian Inc, Wallingford

Iijima S (1991) Helical microtubules of graphitic carbon. Nature 354(6348):56–58

Jianrong C, Yuqing M, Nongyue H, Xiaohua W, Sijiao L (2004) Nanotechnology and biosensors. Biotechnol Adv 22(7):505–518

Lee C, Yang W, Parr RG (1988) Development of the Colle-Salvetti correlation-energy formula into a functional of the electron density. Phys Rev B 37(2):785–789

Liu Z, Liang X-J (2012) Nano-carbons as theranostics. Theranostics 2(3):235–237

Liu P, Wei Y, Liu K, Liu L, Jiang K, Fan S (2012) New-type planar field emission display with superaligned carbon nanotube yarn emitter. Nano Lett 12(5):2391–2396

Mammino L, Kabanda MM (2009) A computational study of the effects of different solvents on the characteristics of the intramolecular hydrogen bond in acylphloroglucinols. J Phys Chem A 113:15064–15077

Nambiar S, Yeow JT (2011) Conductive polymer-based sensors for biomedical applications. Biosens Bioelectron 26(5):1825–1832

Parr RG, Lv Szentpaly, Liu S (1999) Electrophilicity index. J Am Chem Soc 121(9):1922–1924

Pearson RG (1988) Absolute electronegativity and hardness: application to inorganic chemistry. Inorg Chem 27(4):734–740

Raissi H, Yoosefian M, Moshfeghi E, Farzad F (2012) Theoretical study on β-aminoacroleine; density functional theory, atoms in molecules theory and natural bond orbitals studies. J Chem Sci 124(3):731–739

Reed AE, Curtiss LA, Weinhold F (1988) Intermolecular interactions from a natural bond orbital, donor-acceptor viewpoint. Chem Rev 88(6):899–926

Ye Y, Ju H (2005) Rapid detection of ssDNA and RNA using multiwalled carbon nanotubes modified screen-printed carbon electrode. Biosens Bioelectron 21(5):735–741

Yoosefian M (2017) Powerful greenhouse gas nitrous oxide adsorption onto intrinsic and Pd doped Single walled carbon nanotube. Appl Surf Sci 392:225–230

Yoosefian M, Etminan N (2016a) Density functional theory (DFT) study of a new novel bionanosensor hybrid; tryptophan/Pd doped single walled carbon nanotube. Physica E 81:116–121

Yoosefian M, Etminan N (2016b) The role of solvent polarity in the electronic properties, stability and reactivity trend of a tryptophane/Pd doped SWCNT novel nanobiosensor from polar protic to non-polar solvents. RSC Adv 6(69):64818–64825

Yoosefian M, Mola A (2015) Solvent effects on binding energy, stability order and hydrogen bonding of guanine–cytosine base pair. J Mol Liq 209:526–530

Yoosefian M, Ansarinik Z, Etminan N (2016) Density functional theory computational study on solvent effect, molecular conformations, energies and intramolecular hydrogen bond strength in different possible nano-conformers of acetaminophen. J Mol Liq 213:115–121